

## Research Article

# Rheological Properties and Microscopic Characterization of Delayed Decay-Modified Asphalt Based on UV Ageing

Hening Gu,<sup>1</sup> Yongqiang Zhu,<sup>2</sup> Yunchu Zhu,<sup>1</sup> Lijing Chu ,<sup>3</sup> Qinyuan Peng,<sup>1</sup> and Qian Chen <sup>4</sup>

<sup>1</sup>School of Civil and Transportation Engineering, Guangdong University of Technology, Guangzhou 510006, China

<sup>2</sup>Guangdong GuanYue Highway & Bridge Co.,Ltd., Guangzhou 511450, China

<sup>3</sup>Guangzhou Urban Planning & Design Survey Research Institute, Guangzhou 510060, China

<sup>4</sup>Key Laboratory of Road Structure & Material of Transport Ministry, Chang'an University, Xi'an 710064, China

Correspondence should be addressed to Qian Chen; 2016121160@chd.edu.cn

Received 10 August 2022; Revised 30 August 2022; Accepted 20 January 2023; Published 6 February 2023

Academic Editor: Meng Guo

Copyright © 2023 Hening Gu et al. This is an open access article distributed under the Creative Commons Attribution License, which permits unrestricted use, distribution, and reproduction in any medium, provided the original work is properly cited.

For clarifying the applying feasibility of hindered amine light stabilizers in asphalt binder, two types of hindered amine light stabilizers were chosen as a UV ageing resistance modifier and the modified asphalt was prepared with a selected UV ageing resistance modifier. The ultraviolet aging testing method of asphalt materials was proposed for UV ageing behavior characterization. Under the condition of different frequencies, the impact of UV ageing resistance modifier on asphalt was investigated through using the frequency sweep test of DSR. Under the effect of ultraviolet aging, the variation of thermal properties of UV ageing resistance-modified asphalt was deeply analyzed by means of a temperature scanning test of DSR following the increase of temperature. The change law of the surface morphology of light stabilizer-modified asphalt was characterized by atomic force microscopy (AFM) dynamically with the UV aging time extension. The research results showed that the hindered amine light stabilizer could improve the high temperature performance of asphalt and achieve the UV aging behavior of asphalt materials effectively. Meanwhile, the corresponding reaction mechanism was explored at the microscopic level.

## 1. Introduction

Intense UV radiation would induce and encourage the aging of asphalt pavements, which is one of the most challenging issues in the field of pavement construction [1, 2]. For mitigating the ultraviolet aging behavior of asphalt material, the common and effective method is to add antiultraviolet aging additives to the asphalt binder [3, 4]. The commonly used antiultraviolet additives are carbon black, AW, and BLE [5, 6]. Most of them are added to modified asphalt to enhance its performance. There are relatively many studies on adding certain kinds of antiultraviolet additives to modified asphalt to enhance its anti-ultraviolet ability, and there are many kinds of additives currently used to achieve the UV ageing resistance performance of asphalt [7, 8]. The study found that the addition of 0.8% carbon black can maximize the antirutting factor of asphalt [9, 10]. However, in the

direct tensile test, it was found that the carbon black would impair the low-temperature performance; therefore, the content of carbon black should be controlled within 0.8% [11]. Relevant studies have found that adding BLE, AW, carbon black, etc., could lead to a good UV ageing resistance property of different types of asphalt, but the applicability of these additives on the SBR modified asphalt is the best [12–14]. The addition of 0.8% AW and BLE has better antiageing properties.

In recent years, some research was performed on hindered amine light stabilizers and modified asphalt, but the degradation of low-temperature performance of asphalt after adding modifiers is still blank [15–17]. Related studies have found that asphalt with hindered amine light stabilizers exhibits the highest strain energy density in the direct tensile test (D T), representing the best low-temperature crack resistance [18, 19]. The light stabilizer asphalt exhibits

excellent performance, because the generated free radicals related to the ultraviolet aging of asphalt will be captured by the nitroxide radicals generated by hindered amines to a certain extent, and this reaction directly enhances the stability of the asphalt [20, 21]. Some scholars have studied the modified asphalt with the hindered amine light stabilizer GW-944 [22]. The study found that the additive could hardly affect the thermal and fatigue performance of asphalt after UV ageing treatment, but it can achieve the improvement of the low-temperature property of asphalt materials [22, 23]. The study also found that the additive should not be incorporated into the base asphalt, and the test results suggested that the UV ageing resistance modifier should be used into SBS- and SBR-modified asphalt [22, 23].

Therefore, two types of HALS light stabilizers were chosen as the UV ageing resistance modifier and modified asphalt was prepared with a selected UV ageing resistance modifier. The ultraviolet aging testing method of asphalt materials was proposed for UV ageing behavior characterization. Under the condition of different frequencies, the impact of UV ageing resistance modifier on asphalt was investigated through using the frequency sweep test of DSR. Under the effect of ultraviolet aging, the variation of thermal properties of UV ageing resistance modified asphalt was deeply analyzed by means of temperature scanning test of DSR following the increase of temperature.

## 2. Materials and Methods

### 2.1. Materials

*2.1.1. Binder.* 70# base asphalt was used to prepare UV ageing resistance-modified asphalt in this study. The physical performances of 70# asphalt are tested and demonstrated in Table 1.

*2.1.2. Modifier.* This study chose hindered amine light stabilizers as the UV ageing resistance modifier to prepare modified asphalt. The models of hindered amine light stabilizers were Tinuvin770 and 622, whose applying dosages were 2%, 4%, and 6% by the asphalt mass. The purity of T770 and T662 was approximately 95%.

*2.2. Preparing Procedure of HALS-Modified Asphalt.* The 70# asphalt was heated and kept around 130°C. The specific weight of HALS was put into the container for use. The HALS modifier was divided into three parts of equal weight and mixed into asphalt for three times. After adding each modifier, the mixture of asphalt was mixed by the high-speed shearing instrument at 1000 rad/min for 15 min. After stirring, the preparation of UV ageing resistance-modified asphalt was finished. The development time of modified asphalt was approximately 12 h.

### 2.3. Test Method

*2.3.1. UV Ageing Method.* In this study, the indoor accelerated UV ageing was performed to treat the HALS-

TABLE 1: Physical property of 70# binder.

Physical property	Indices value	Specification
Softening point (°C)	49.2	>43
Penetration (0.1 mm)	70.3	60~80
10°C ductility (cm)	26.5	>15

modified asphalt for UV ageing. The ultraviolet radiation powder was about 300 W. Furthermore, the size of UV radiation was about 0.8 m<sup>2</sup> and the average ultraviolet radiation was approximately 375 W/m<sup>2</sup>. Through energy equation calculation by formula (1), the indoor UV treatment times mainly included 76.25 h, 152.5 h, 228 h, and 305 h.

$$\text{Indoor simulation time} = \frac{\text{Outdoor solar radiation energy}}{\text{Power of indoor UV radiation}} \quad (1)$$

### 2.3.2. Rheological Property Characterization

*(a) Frequency Sweeping.* Anton Paar MCR 302 rheometer was used in this study (Figure 1). The strain controlling mode was chosen for the frequency sweeping test to performed the DSR test. The strain was controlled around 1% and the sweeping frequency was from 0.1 rad/s to 100 rad/s [24]. The test temperature of the frequency sweeping test was from 25°C to 70°C. Among them, a 8 mm parallel plate was used at 25°C and the spacing was controlled to 2 mm. At 40°C~70°C, a 25 mm parallel plate was used, and the spacing is controlled to 1 mm.

*(b) Temperature Sweeping.* The control strain of the temperature sweep test was 12%. The test frequency was 10 rad/s. A 25 mm parallel plate was used for testing with 1 mm spacing. The test temperature range was from 46°C to 82°C and the heating interval was 6°C. Five data points were taken for each set temperature and averaged.

*(c) Bending Beam Rheological Test.* The experimental test was carried out using the TE-BBR bending beam rheometer (Figure 1) manufactured by Cannon. According to the ASTM D6648-01 [25] test method, the test temperature was -12°C.

*2.3.3. AFM Analysis.* The Dimension FastScan scanning probe microscope (Figure 2) was used to observe the microscopic morphology of UV aged modified asphalt. The microtopography of the sample surface was scanned by the fast scanning head. The probe used was the silicon nitride cantilever probe [26].

## 3. Results and Discussion

### 3.1. Frequency Sweep Test Results

*3.1.1. Rheological Properties under Specific Frequency Conditions.* Figures 3–5 are the curves of the complex shear

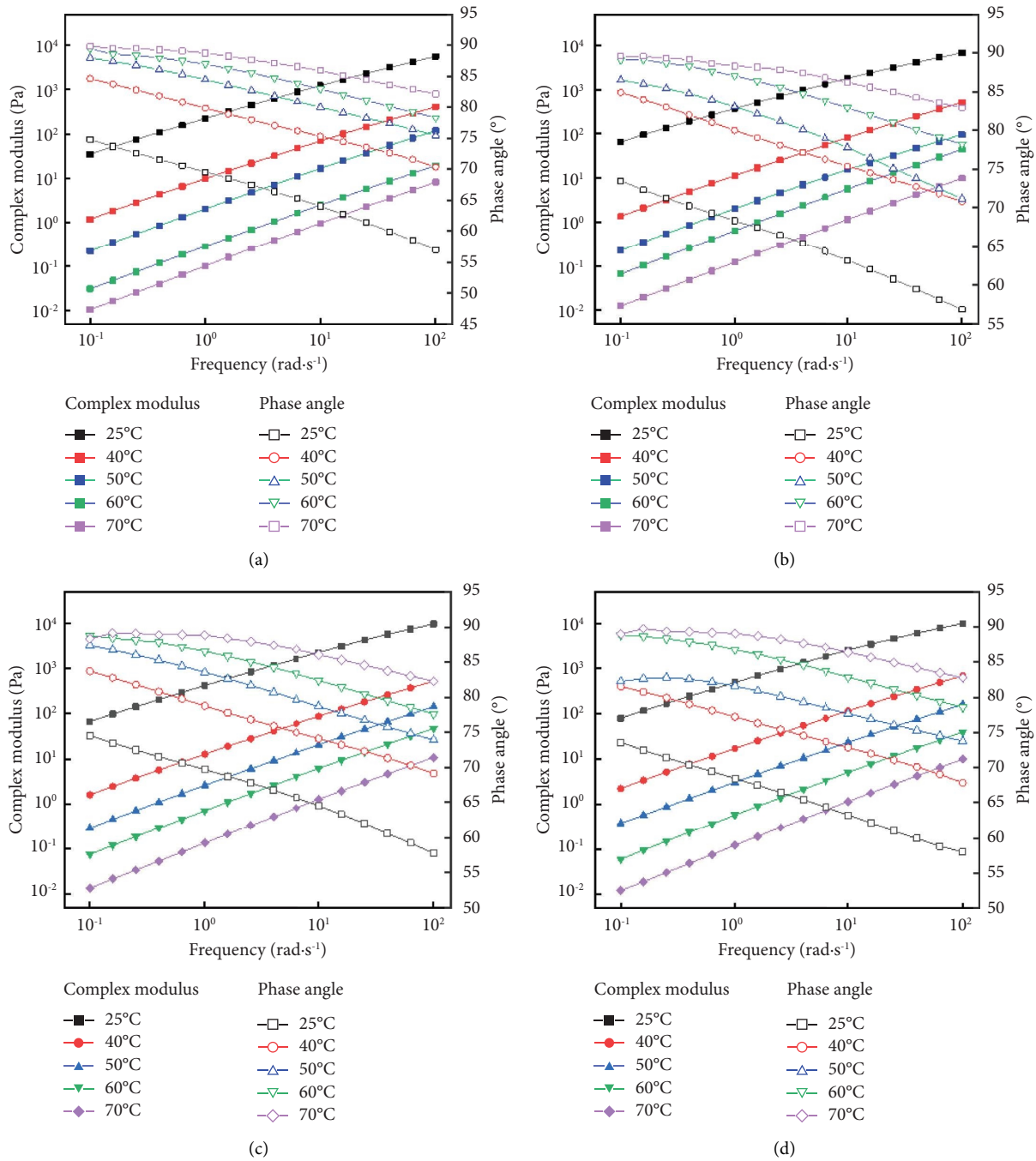


FIGURE 1:  $G^*$  and  $\delta$  change curves of 70# asphalt under different aging times. (a) 76.25 h. (b) 152.5 h. (c) 228 h. (d) 305 h.

modulus and the phase angle of modified asphalt following the variation of frequency under different aging times. From the analysis of Figures 1–4, with the increase of temperature,  $G^*$  of different asphalts decreased, while the phase angle increased, which reflected that asphalt had stronger fluidity at high temperature, and the resistance to deformation of asphalt material degraded. When the temperature gradually increased, the  $G^*$  of modified asphalt was similar to that of the 70# asphalt, which demonstrated that the  $G^*$  of the 70# asphalt was relatively less affected by the light stabilizer at higher temperatures.

**3.1.2. Rheological Properties under Specific Temperature Conditions.** Figures 5 and 6 are the graphs of the  $G^*$  and  $\delta$  of modified asphalt at 40°C and 60°C following the variation of frequency under different aging time conditions, respectively. From Figures 5 and 6, after the UV aging treatment, the  $G^*$  of modified asphalt increased, while the  $\delta$  decreased. For 70# asphalt, the  $G^*$  increased and  $\delta$  decreased following the extension of UV aging time. This showed that the elastic component in the internal viscoelastic composition of the asphalt material increased during the UV ageing process, and the deformation resistance property of asphalt

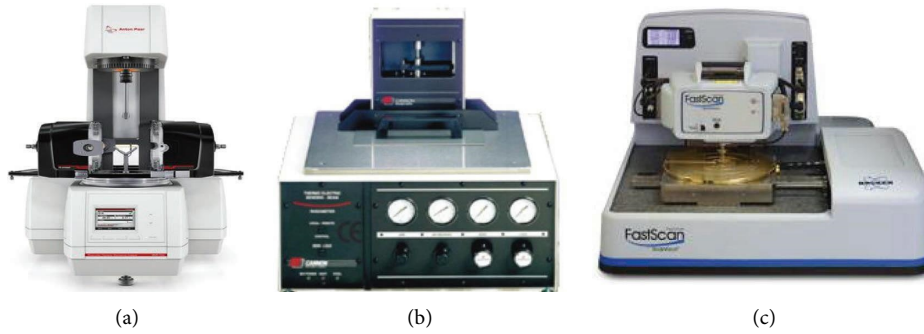


FIGURE 2: Testing equipment. (a) Anton Paar MCR 302. (b) TE-BBR. (c) Dimension FastScan.

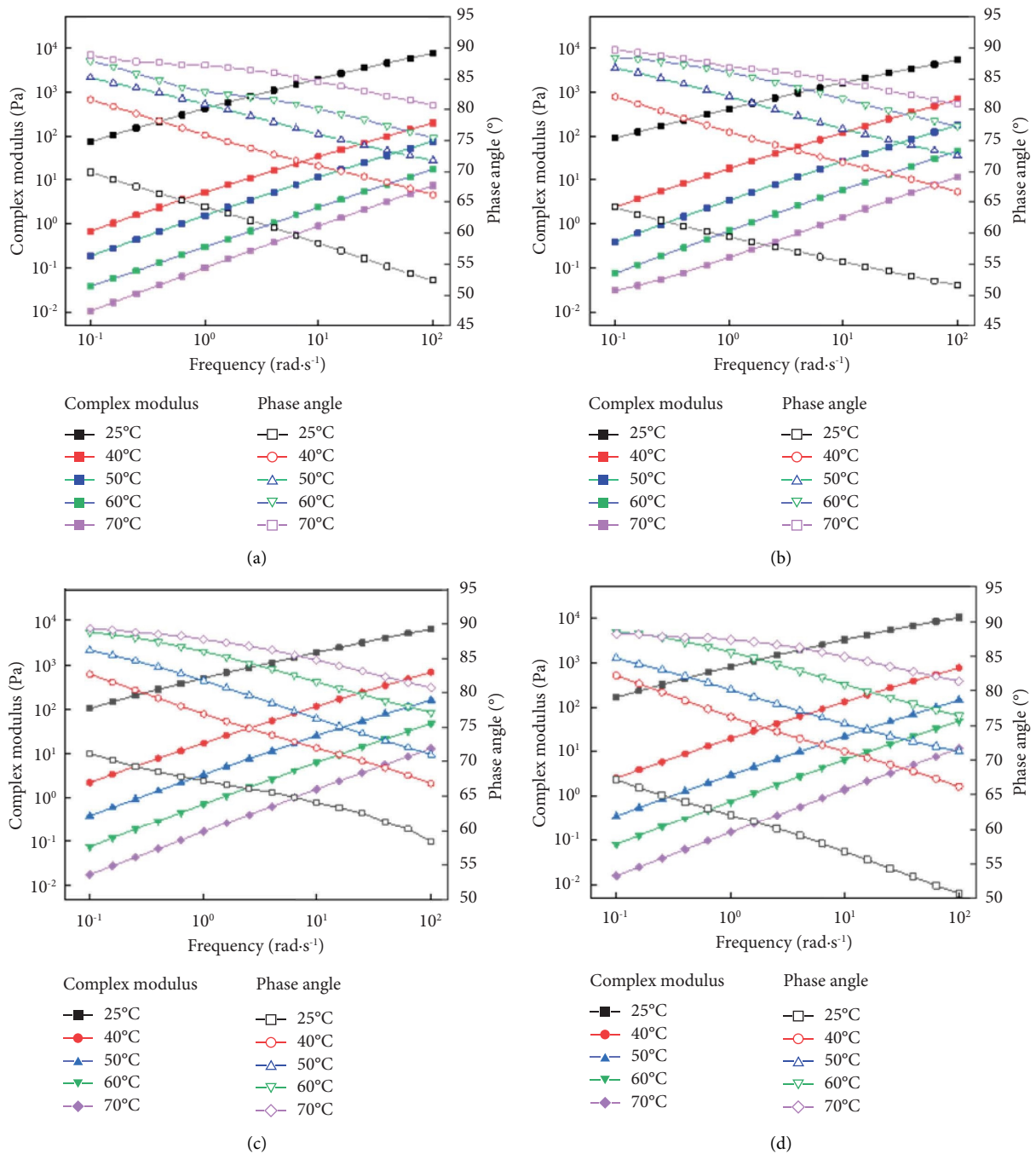


FIGURE 3:  $G^*$  and  $\delta$  change curves of T770 modified asphalt under different aging times. (a) 76.25 h. (b) 152.5 h. (c) 228 h. (d) 305 h.

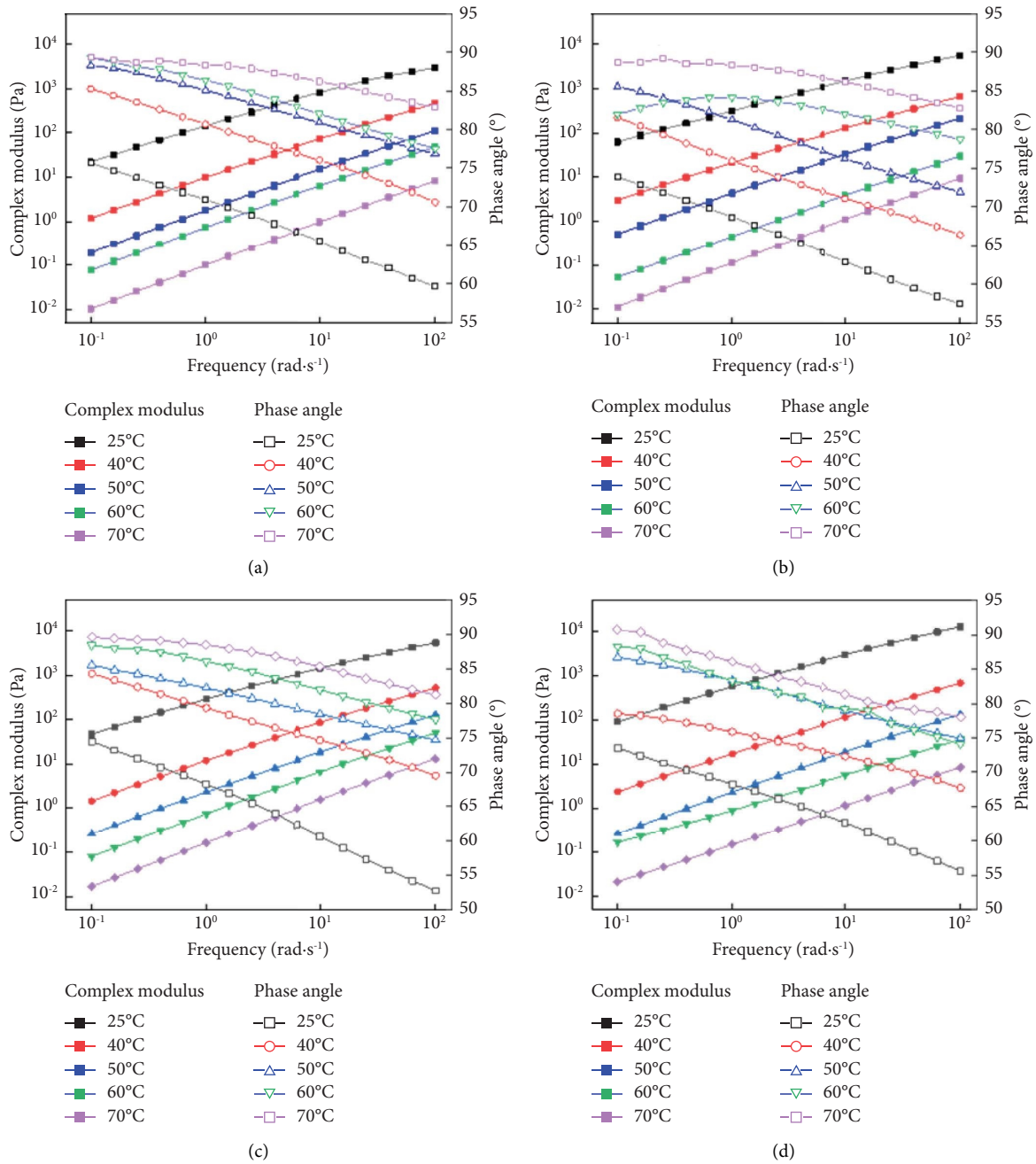


FIGURE 4:  $G^*$  and  $\delta$  change curves of T622 modified asphalt under different aging times. (a) 76.25 h. (b) 152.5 h. (c) 228 h. (d) 305 h.

material was enhanced significantly, whose macroscopic performance was enhanced at high temperature. When the UV ageing time increased from 76.25 h to 152.5 h at 60°C, the  $G^*$  of T770 asphalt decreased while  $\delta$  increased, which supposed that the elastic component of asphalt was reduced and the deformation resistance was weakened. When the aging time increased from 152.5 h to 228 h and 305 h, the  $G^*$  increased and the  $\delta$  decreased. This changing phenomenon

might be related to the improvement of deformation resistance of the asphalt.

For T622-modified asphalt, the complex shear modulus difference between aging 152.5 h, 228 h, and 305 h was small, which were higher than the  $G^*$  of asphalt aged 76.25 h. Compared with 70# asphalt, the  $G^*$  of T622-modified asphalt aged 76.25 h was smaller than that of 70# asphalt, while the  $\delta$  was larger than 70# asphalt. When aged 152.5 h, 228 h,

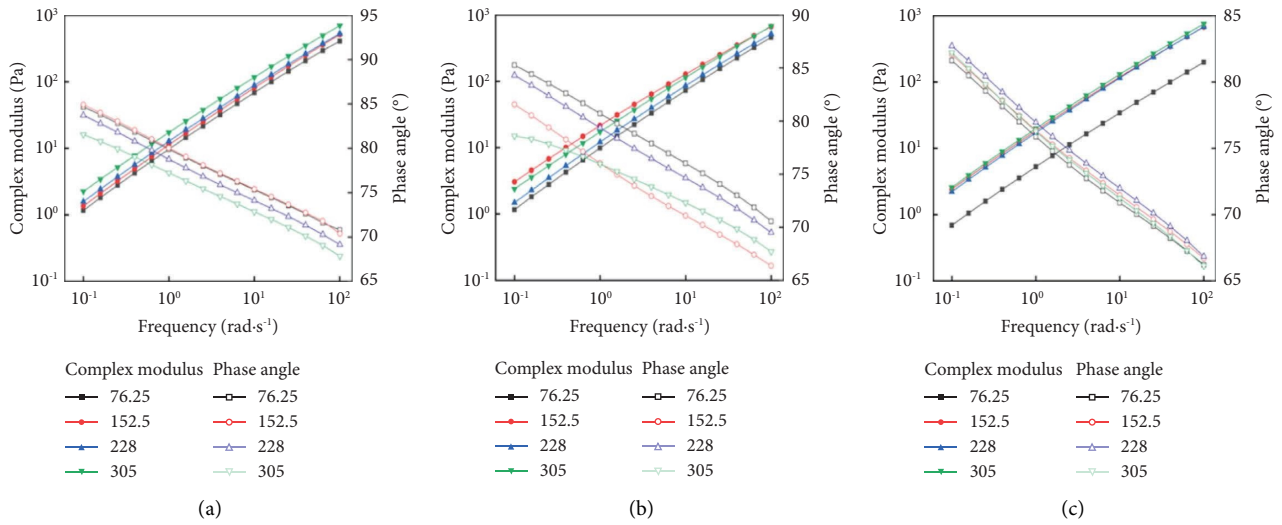


FIGURE 5: Variation curves of  $G^*$  and  $\delta$  of different types of asphalt with UV aging time at 40°C. (a) 70#. (b) T770. (c) T622.

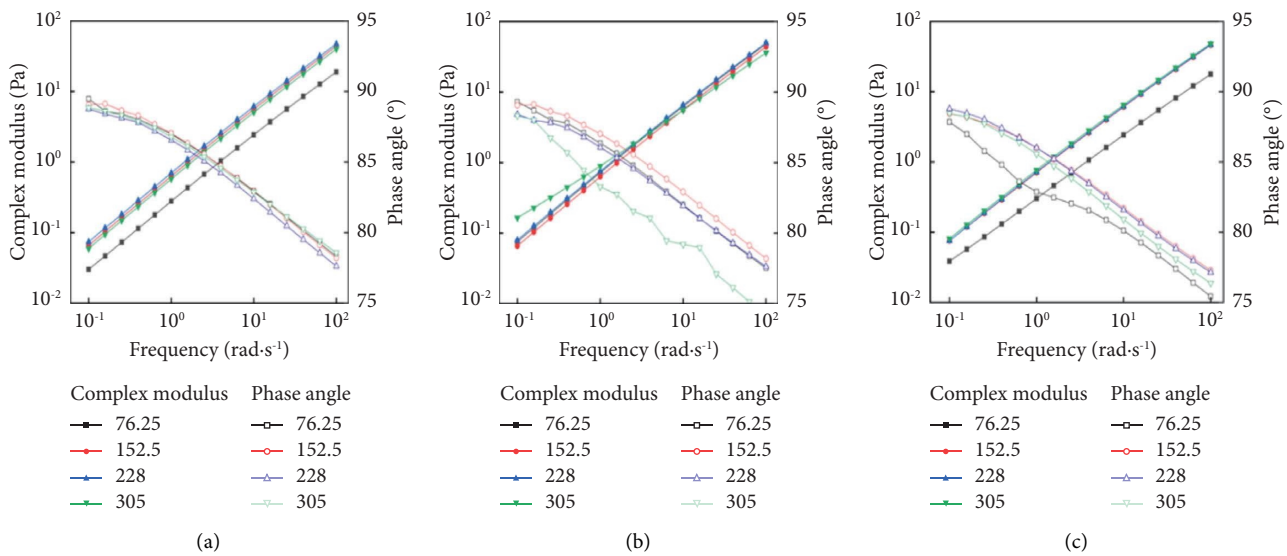


FIGURE 6: Variation curves of  $G^*$  and  $\delta$  of different types of asphalt with UV aging time at 60°C. (a) 70#. (b) T770. (c) T622.

and 305 h, the  $G^*$  of T622-modified asphalt and 70# asphalt were not much different. To sum up, the T622 modifier and T770 modifier could mitigate the UV aging process of asphalt and T622 modifier had a better improvement effect. However, as the aging time was gradually prolonged, the modification effect would decrease.

**3.2. Temperature Sweep Test Results.** Figure 7 shows the results of the temperature sweep phase angle test of 70# base asphalt and light stabilizer-modified asphalt, respectively. It could be seen from the analysis that the  $\delta$  of modified asphalt rose with the temperature, supposing that the viscosity of the asphalt increased while the elasticity decreased. At the same time, it could be found that when UV aging time extended,

the  $\delta$  of asphalt decreased, which proved that UV radiation might promote the elastic response of asphalt, and the enhancing effect was improved with the prolongation of irradiation time. It was worth noting that the  $\delta$  of modified asphalt decreased with time, which demonstrated that the HALS could lead to the UV aging resistant effect on asphalt.

From Figure 8, with the time extension of UV ageing, the  $G^*$  of asphalt increased, indicating that the asphalt material is hardened to different degrees after UV irradiation, and the deformation resistance is enhanced. Compared with the base asphalt, the  $G^*$  growth rate of the light stabilizer-modified asphalt had decreased significantly, which proved that the light stabilizer-modified asphalt had an excellent UV ageing resistant performance. At the same time, it was found that when the aging time was within 76.25~152.5 h, the difference

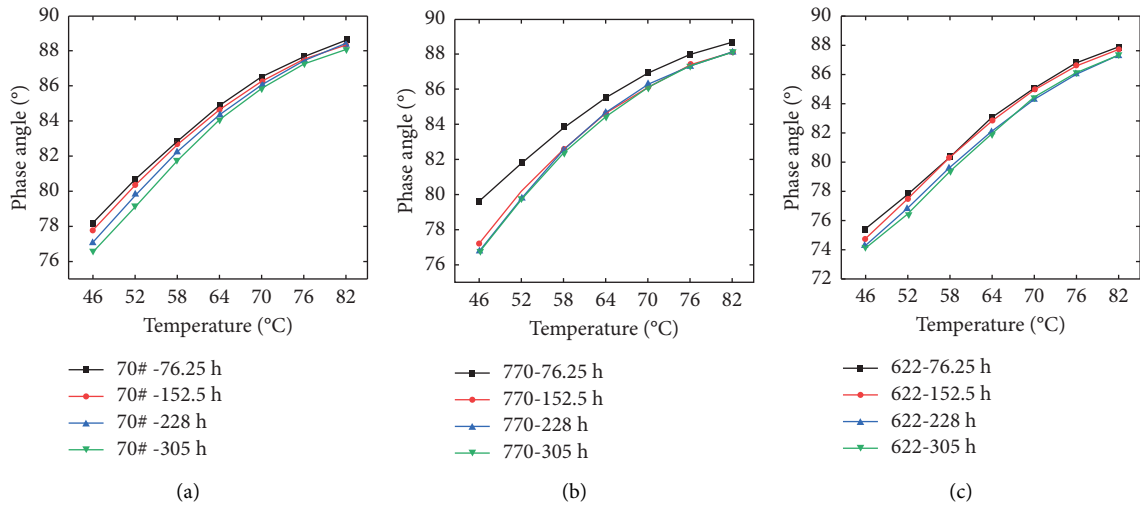


FIGURE 7:  $\delta$  variation curves of different types of asphalt with UV aging time (a) 70#. (b) T770. (c) T622.

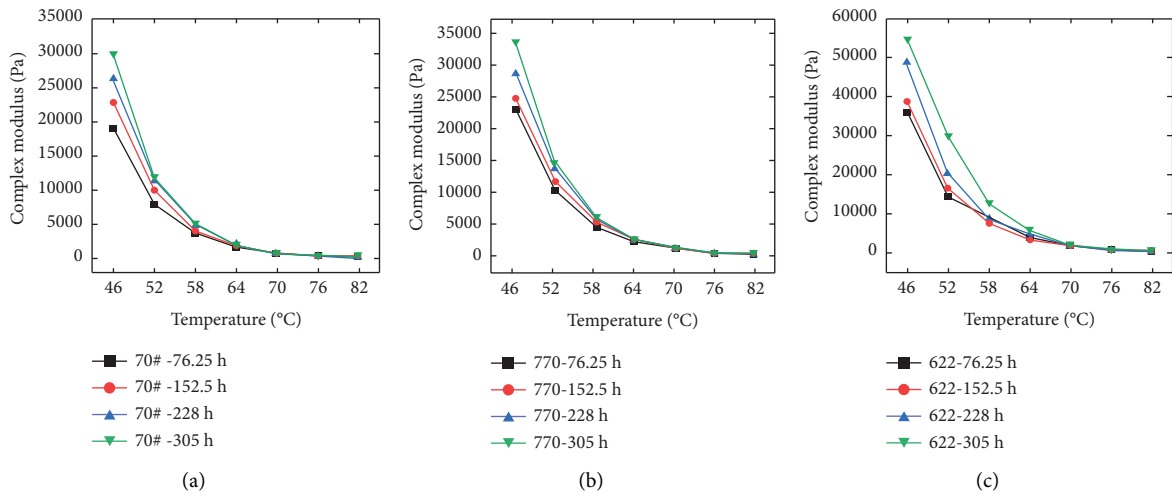


FIGURE 8:  $G^*$  variation curves of different types of asphalt with UV aging time. (a) 70#. (b) T770. (c) T622.

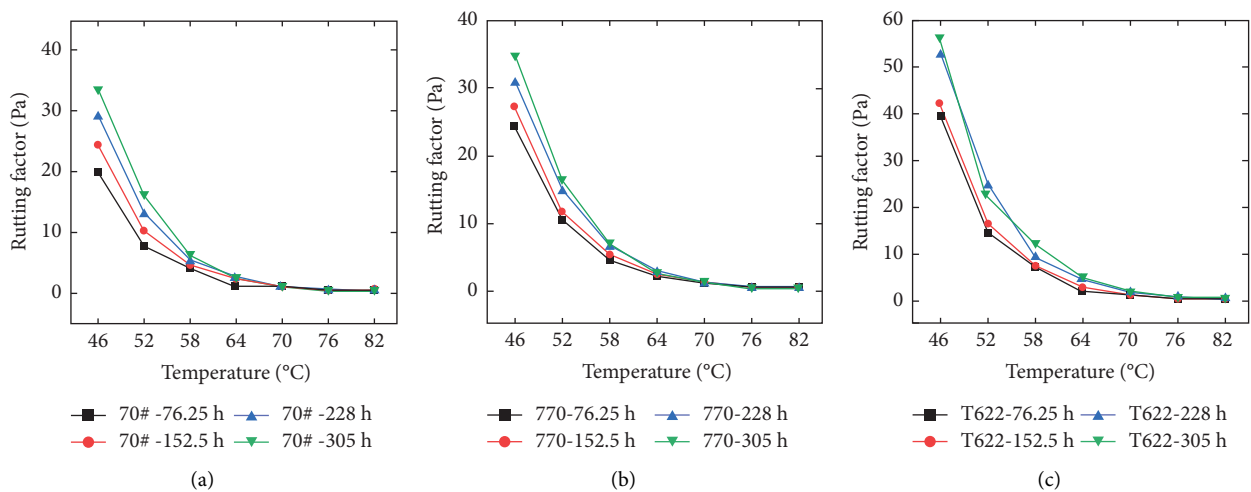


FIGURE 9: Rutting factor variation curves of different types of asphalt with UV aging time. (a) 70#. (b) T770. (c) T622.

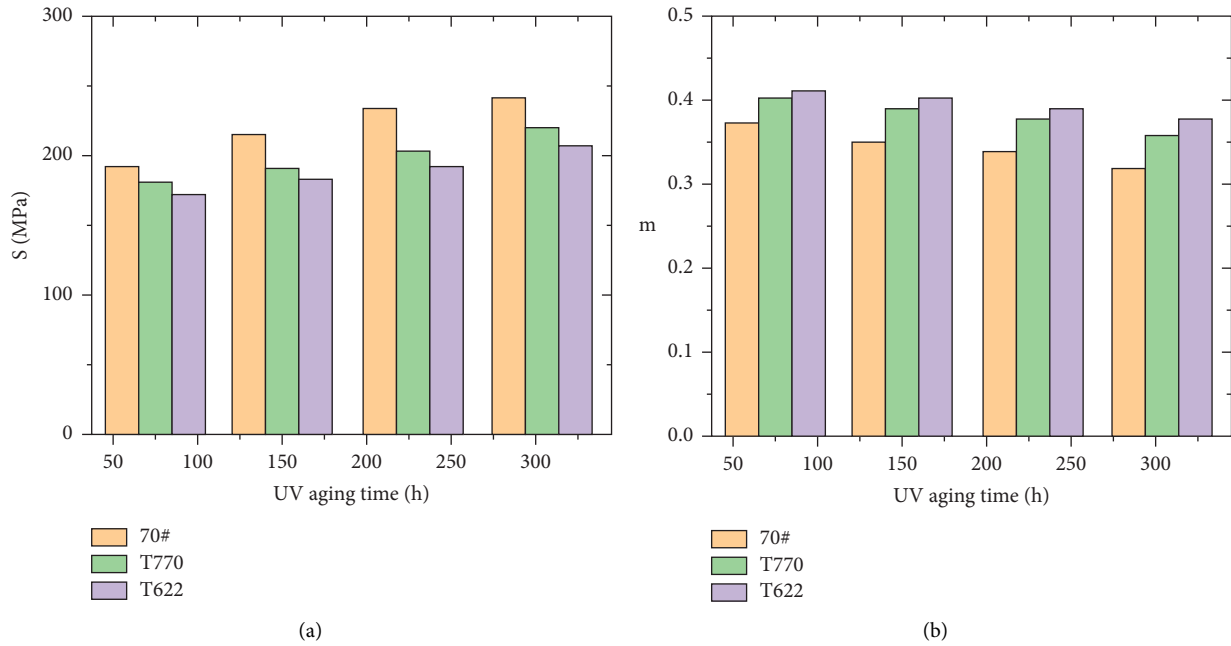


FIGURE 10: BBR testing results. (a)  $S$ . (b)  $m$ .

in complex modulus between T770 and T622-modified asphalt was small. With the time extension of UV ageing treatment, the difference in the  $G^*$  of asphalt was becoming obvious. The asphalt hardness was significantly improved, which indicated that the effect of ultraviolet rays on the asphalt hardness was light at the beginning. When the UV aging time continued prolonging, this effect increased significantly, which led to the significant increase in asphalt hardness.

Figure 9 presents the rutting factors of 70# asphalt and modified asphalt. From Figure 9, the rutting factor had the similar variation law to the  $G^*$  and increased with the time extension of UV aging treatment. Furthermore, with the time extension of UV, the improving effect of rutting factor was strengthened. Compared with 70# asphalt, the difference in rutting factor between T770 and T622-modified asphalt was smaller between 76.25 h and 152.5 h. As the UV aging progressed, the asphalt exhibited different degrees of aging, manifested as the decrease in the  $\delta$ , and the increase in the rutting factor and  $G^*$ , which meant that the elasticity and hardness of the asphalt increased gradually. The UV aging degree of modified asphalt was obviously less than that of 70# asphalt, which proved that HALS could mitigate the UV aging degree of asphalt material.

**3.3. Bending Beam Rheological Test Results.** Figure 10 demonstrates the rheological test results of BBR bending beams. From the analysis in Figure 10, it could be seen that the  $S$  of modified asphalt was less than 70# asphalt, and the  $S$  was greater than that of 70# asphalt. With the gradual time extension of UV ageing treatment, the  $S$  of modified asphalt increased, while the  $m$  decreased, which supposed that the time extension of UV aging treatment degraded the low-

temperature performance of asphalt materials. For 70# asphalt, when the UV aging time extended from 76.25 h to 305 h, the  $S$  increased by 12%, 21%, and 25%, and the  $m$  decreased by 6%, 11%, and 15%. The varying rate of  $S$  and  $m$  of T622-modified asphalt was obviously smaller than 70# asphalt. The performance index of T770-modified asphalt showed the similar law to that of T622-modified asphalt. Therefore, it could be judged that both HALS could mitigate the influence of ultraviolet light on road performance of asphalt materials.

**3.4. AFM Analysis.** The AFM morphology of 70# asphalt is shown in Figure 11. After 76.25 h of aging, the surface of 70# asphalt tended to be circular, and other rod-like and rectangular structures existed. After aging for 152.5 h, the number of circular structures on the surface was significantly reduced, and the surface mostly existed in rod-like morphology. The overall surface morphology was more complex. After 228 h of aging, dark structures with the height of around  $1 \mu\text{m}$  in the middle and the size of more than  $1 \mu\text{m}$  appeared on the surface. Apart from this structure, the rest of the surface was relatively smooth. After aging for 305 h, the original small and dense point-like structure appeared on the asphalt surface, and the aggregated area of the structure had higher roughness.

The AFM results of T770-modified asphalt are shown in Figure 12. After UV aging for 76.25 h, many rod-like structures with a length of about  $1 \mu\text{m}$  appeared on T770 asphalt. The rod-like structure was characterized by the high middle and low ends, while the roughness of the asphalt surface increased. In addition, there were scattered domains around the structure, and the highlighted structure indicated that its height was higher than that of the 70# asphalt. After



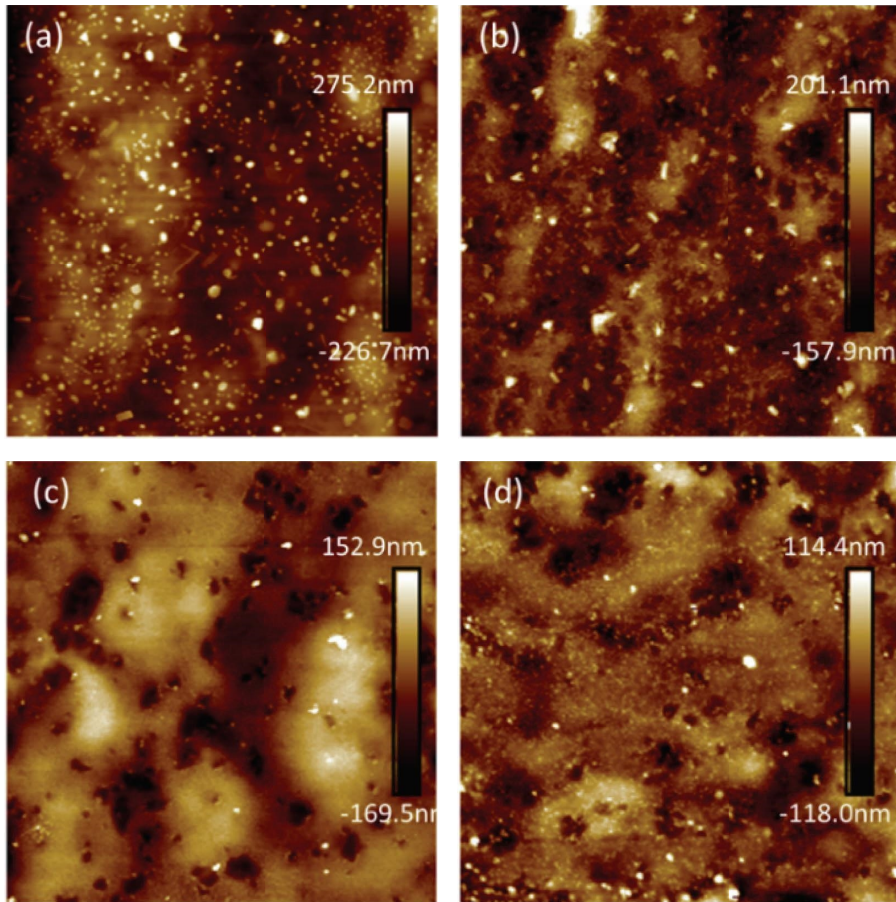


FIGURE 11: AFM images of 70# asphalt. (a) 76.25 h. (b) 152.5 h. (c) 228 h. (d) 305 h.

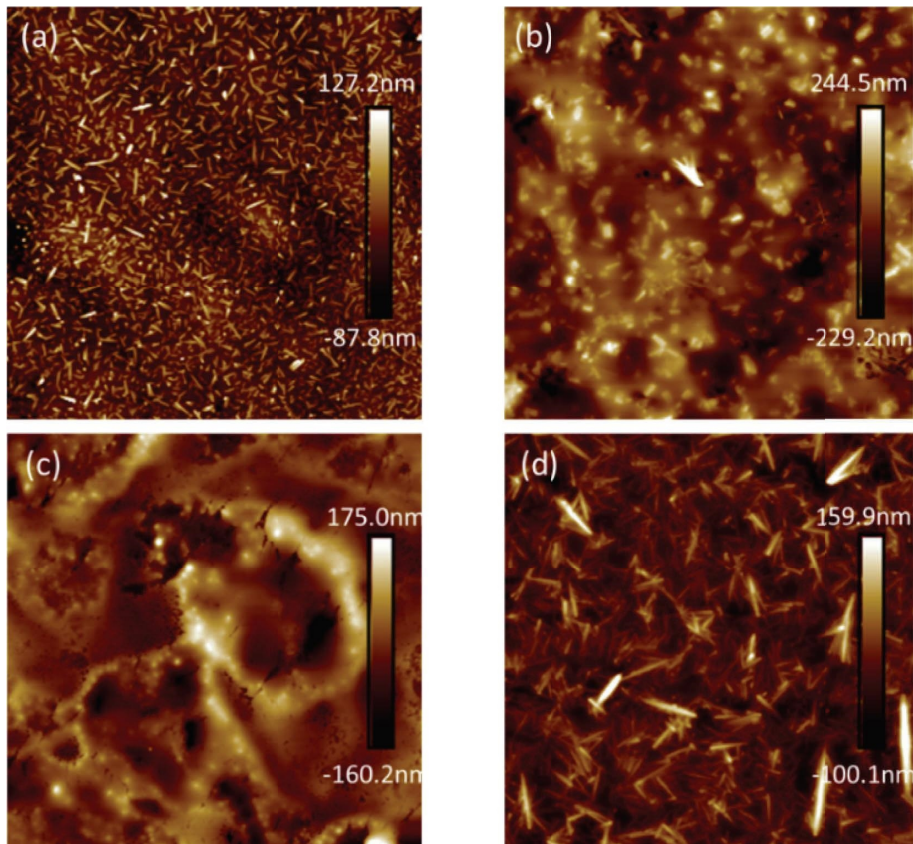


FIGURE 12: AFM images of T770 modified asphalt. (a) 76.25 h. (b) 152.5 h. (c) 228 h. (d) 305 h.

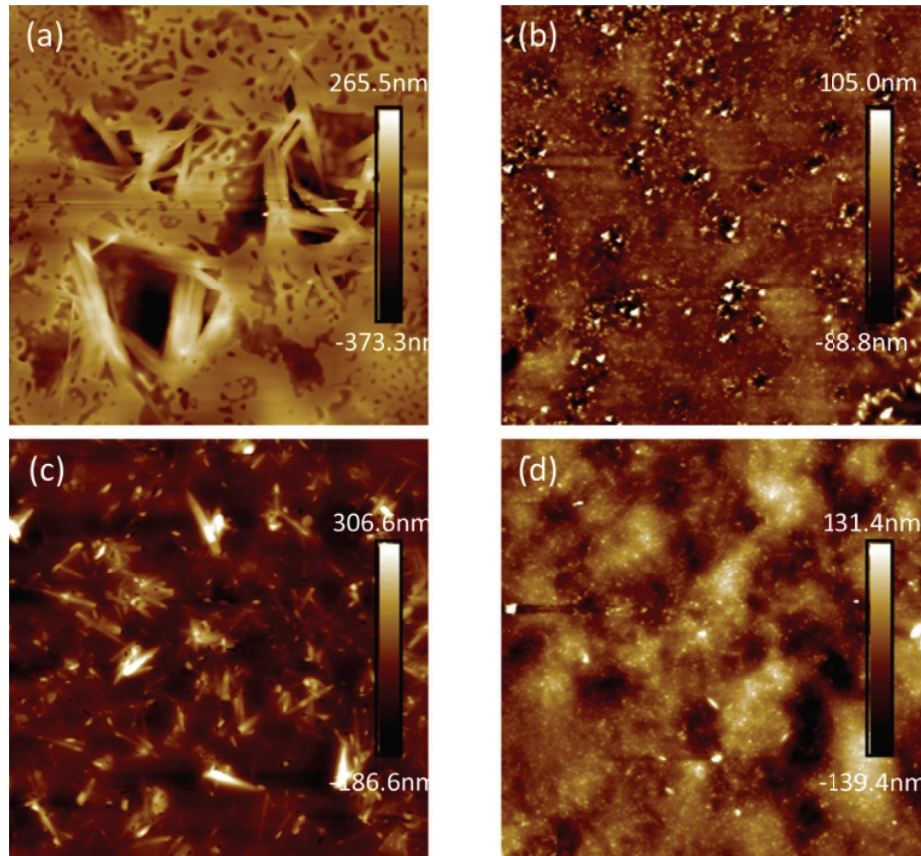


FIGURE 13: AFM images of T622 modified asphalt. (a) 76.25 h. (b) 152.5 h. (c) 228 h. (d) 305 h.

152.5 hours, the surface of the asphalt was distributed with high-brightness rod-like structures, while the width of the structure was wider compared to that of 76.25 h. However, the length was relatively short, generally within  $1\ \mu\text{m}$ . After 228 h of aging, the rod-like structure disappeared and was replaced by the smaller and smoother microbright structure with the average length of about 300 nm. After 305 h aging, the rod-like structure reappeared, the length increased significantly, and the asphalt surface roughness increased significantly.

The AFM results of T622 modified asphalt are shown in Figure 13. After aging for 76.25 h, the surface roughness of T622 asphalt increased, and there were concave structures among the special structures. After 152.5 hours of aging, the cluster structure appeared on the asphalt surface in the form of blocks, and the surface roughness increased. After 228 h of aging, the rod-like structure appeared again. The structure was still characterized by the elongated shape.

#### 4. Conclusions

- (i) As the temperature increased, the  $G^*$  of different pitches decreased and the  $\delta$  increased, which reflected that the ability of asphalt materials to resist deformation was weakened.
- (ii) T622 and T770 modifiers could effectively mitigate the UV aging process of asphalt and the improving effect of T622 modifier was better. But as the aging

time gradually prolonged, its modifying effect might be degraded.

- (iii) Following the UV ageing time extension, the  $S$  of HALS-modified asphalt was both smaller than base asphalt and the  $m$  was obviously greater than 70# asphalt, which supposed that HALS could prevent the degradation of the low-temperature property of asphalt when subjected to UV radiation.
- (iv) When subjected to the UV radiation, the surface of HALS-modified asphalt mainly had a rod-like structure as the main microstructure, and with the time extension of UV aging treatment, the microstructure would go through relatively complex changes.

#### Data Availability

The data used to support the findings of this study are available from the corresponding author upon request.

#### Conflicts of Interest

The authors declare that they have no conflicts of interest.

#### Acknowledgments

This study was supported by the Open Fund of National Engineering Research Center of Highway Maintenance

Technology (Changsha University of Science&Technology) (kfj220104), the Fundamental Research Funds for the Central Universities under (grant no. 300102212516), the Open Research Fund of Highway Engineering Key Laboratory of Sichuan Province, Southwest Jiaotong University (HEKLSP2022-8), Special Fund for Science and Technology Innovation Strategy of Guangdong Province under (grant nos. pdjh2021a0149 and pdjh2022b0161), and Guangdong GuanYue Highway & Bridge Co., Ltd. Enterprise Mission Project under (grant no. GDKTP2021009700).

## References

- [1] S. Yang, K. Yan, and W. Liu, "The effect of ultraviolet aging duration on the rheological properties of sasobit/SBS/Nano-TiO<sub>2</sub>-Modified asphalt binder," *Applied Sciences*, vol. 12, no. 20, Article ID 10600, 2022.
- [2] H. Yu, Z. Leng, Z. Zhou, K. Shih, F. Xiao, and Z. Gao, "Optimization of preparation procedure of liquid warm mix additive modified asphalt rubber," *Journal of Cleaner Production*, vol. 141, pp. 336–345, 2017.
- [3] H. Zhang and D. Zhang, "Effect of different inorganic nanoparticles on physical and ultraviolet aging properties of bitumen," *Journal of Materials in Civil Engineering*, vol. 27, no. 12, Article ID 04015049, 2015.
- [4] X. Sun, X. Qin, Z. Liu, Y. Yin, C. Zou, and S. Jiang, "New preparation method of bitumen samples for UV aging behavior investigation," *Construction and Building Materials*, vol. 233, Article ID 117278, 2020.
- [5] H. Liu, Z. Zhang, N. Li, H. Li, and P. Wang, "Effect of organic montmorillonite on rheological properties of sasobit warm-mix asphalt and analysis of its ultraviolet aging behaviors," *Journal of Materials in Civil Engineering*, vol. 34, no. 12, Article ID 04022339, 2022.
- [6] X. Qin and X. Sun, "Quantitative investigation and decision support of reducing effect of warm mixed asphalt mixture (WMA) on emission and energy consumption in highway construction," *Environmental Science and Pollution Research*, vol. 29, no. 22, pp. 33383–33399, 2022.
- [7] B. Yang, H. Li, N. Xie, J. Yang, and J. Liu, "Surface characteristics of ageing asphalt binder coupling thermal oxidation and ultraviolet radiation," *Transportation Research Record*, vol. 2676, Article ID 03611981221088583, 2022.
- [8] J. Jin, Y. Gao, Y. Wu et al., "Rheological and adhesion properties of nano-organic palygorskite and linear SBS on the composite modified asphalt," *Powder Technology*, vol. 377, pp. 212–221, 2021.
- [9] J. Jin, Y. Gao, Y. Wu et al., "Performance evaluation of surface-organic grafting on the palygorskite nanofiber for the modification of asphalt," *Construction and Building Materials*, vol. 268, Article ID 121072, 2021.
- [10] H. Yu, Z. Zhu, Z. Leng et al., "Effect of mixing sequence on asphalt mixtures containing waste tire rubber and warm mix surfactants," *Journal of Cleaner Production*, vol. 246, Article ID 119008, 2020.
- [11] X. An, R. Wang, X. Kang, and J. Yue, "A more accurate fatigue characterization of GO-modified asphalt binder considering non-linear viscoelastic behaviour and UV exposure effects," *International Journal of Fatigue*, vol. 168, Article ID 107396, 2023.
- [12] M. Guo, M. Liang, Y. Jiao, W. Zhao, Y. Duan, and H. Liu, "A review of phase change materials in asphalt binder and asphalt mixture," *Construction and Building Materials*, vol. 258, Article ID 119565, 2020.
- [13] Chen, C. Wang, Y. Li, L. Feng, and S. Huang, "Performance development of polyurethane elastomer composites in different construction and curing environments," *Construction and Building Materials*, vol. 365, Article ID 130047, 2023.
- [14] P. Cong, X. Wang, P. Xu, J. Liu, R. He, and S. Chen, "Investigation on properties of polymer modified asphalt containing various antiaging agents," *Polymer Degradation and Stability*, vol. 98, no. 12, pp. 2627–2634, 2013.
- [15] S. Lv, X. Peng, C. Liu et al., "Aging resistance evaluation of asphalt modified by Buton-rock asphalt and bio-oil based on the rheological and microscopic characteristics," *Journal of Cleaner Production*, vol. 257, Article ID 120589, 2020.
- [16] M. Guo, M. Liang, A. Sreeram, A. Bhasin, and D. Luo, "Characterization of rejuvenation of various modified asphalt binders based on simplified chromatographic techniques," *International Journal of Pavement Engineering*, vol. 23, pp. 1–11, 2021.
- [17] Q. Chen, C. Wang, S. Yu, Z. Song, H. Fu, and T. An, "Low-temperature mechanical properties of polyurethane-modified waterborne epoxy resin for pavement coating," *International Journal of Pavement Engineering*, pp. 1–13, 2022.
- [18] H. Yu, X. Bai, G. Qian et al., "Impact of ultraviolet radiation on the aging properties of SBS-modified asphalt binders," *Polymers*, vol. 11, no. 7, p. 1111, 2019.
- [19] M. Gao, C. Fan, X. Chen, and M. Li, "Study on ultraviolet aging performance of composite modified asphalt based on rheological properties and molecular dynamics simulation," *Advances in Materials Science and Engineering*, vol. 2022, Article ID 7894190, 9 pages, 2022.
- [20] M. Guo, X. Liu, Y. Jiao, Y. Tan, and D. Luo, "Rheological characterization of reversibility between aging and rejuvenation of common modified asphalt binders," *Construction and Building Materials*, vol. 301, Article ID 124077, 2021.
- [21] A. Abouelsaad and G. White, "The combined effect of ultraviolet irradiation and temperature on hot mix asphalt mixture aging," *Sustainability*, vol. 14, no. 10, p. 5942, 2022.
- [22] Z. G. Feng, J. Y. Yu, H. L. Zhang, D. L. Kuang, and L. H. Xue, "Effect of ultraviolet aging on rheology, chemistry and morphology of ultraviolet absorber modified bitumen," *Materials and Structures*, vol. 46, no. 7, pp. 1123–1132, 2013.
- [23] S. Li, W. Xu, F. Zhang, H. Wu, and Q. Ge, "Effect of graphene oxide on aging properties of polyurethane-SBS modified asphalt and asphalt mixture," *Polymers*, vol. 14, no. 17, p. 3496, 2022.
- [24] X. Sun, Z. Ou, Q. Xu et al., "Feasibility analysis of resource application of waste incineration fly ash in asphalt pavement materials," *Environmental Science and Pollution Research International*, pp. 1–16, 2022.
- [25] Q. Zhang, X. Cai, K. Wu et al., "Shear performance of recycled asphalt mixture based on contact interface parameter analysis," *Construction and Building Materials*, vol. 300, Article ID 124049, 2021.
- [26] X. Sun, Q. Peng, Y. Zhu, Q. Chen, J. Yuan, and Y. Zhu, "Effects of UV aging on physical properties and physicochemical properties of ASA polymer-modified asphalt," *Advances in Materials Science and Engineering*, vol. 2022, Article ID 1157687, 12 pages, 2022.